Journal of Biosciences and Medicines, 2025, 13(11), 161-187
https://www.scirp.org/journal/jbm
ISSN Online: 2327-509X
ISSN Print: 2327-5081

LDHC as a Novel Tumor-Suppressive Biomarker in Cervical Cancer: Multi-Omics Analysis Reveals Diagnostic and Prognostic Significance

Shanshan Xiao[1,2], Yuhong Hu[2], Yawen Li[1,2], Xin Zhang[2], Zijun Xiao[2], Mingyou Dong[2,3*], Lusheng Liao[2,4*]

[1]Department of Obstetrics and Gynecology, The Affiliated Hospital of Youjiang Medical University for Nationalities, Baise, China
[2]Modern Industrial College of Biomedicine and Great Health, Youjiang Medical University for Nationalities, Baise, China
[3]Guangxi Engineering Research Center for Precise Genetic Testing of Long-Dwelling Nationalities, Baise, China
[4]Key Laboratory of Research on Environment and Population Health in Aluminium Mining Areas, Education Department of Guangxi Zhuang Autonomous Region, Baise, China
Email: *mydong@ymun.edu.cn, *01188@ymunedu.cn

How to cite this paper: Xiao, S.S., Hu, Y.H., Li, Y.W., Zhang, X., Xiao, Z.J., Dong, M.Y. and Liao, L.S. (2025) LDHC as a Novel Tumor-Suppressive Biomarker in Cervical Cancer: Multi-Omics Analysis Reveals Diagnostic and Prognostic Significance. *Journal of Biosciences and Medicines*, **13**, 161-187.
https://doi.org/10.4236/jbm.2025.1311012

Received: September 18, 2025
Accepted: November 7, 2025
Published: November 10, 2025

Abstract

This study presents a comprehensive molecular characterization of lactate dehydrogenase (*LDH*) family members in cervical squamous cell carcinoma (CESC). Through integrated multi-omics analysis of TCGA and GEO datasets, we identified distinct tissue-specific expression patterns, with *LDHA* and *LDHB* showing ubiquitous expression while *LDHAL6B* and *LDHC* exhibited testis-specific restriction. Pan-cancer analysis revealed significant overexpression of multiple *LDH* isoforms in CESC and other malignancies, with *LDHC* demonstrating exceptional diagnostic performance (AUC = 0.950 in TCGA, AUC = 0.884 in GSE63514). Survival analysis established *LDHC* as a favorable prognostic marker, contrasting with the poor outcomes associated with other *LDH* isoforms. Functional network analysis revealed *LDH* family involvement in key metabolic pathways including pyruvate metabolism and glycolysis. Epigenetic regulation was implicated through differential methylation patterns, particularly *LDHB* hypermethylation and *LDHC* hypomethylation in tumor tissues. Immune correlation analysis demonstrated significant associations between *LDH* expression and immune cell infiltration/checkpoint markers. Crucially, functional validation in Hela cells showed that *LDHC* knockdown enhanced proliferation (CCK-8 assay), colony formation, migration (wound

healing), and invasion (Transwell), suggesting a tumor-suppressive role. These findings establish *LDHC* as a promising diagnostic biomarker and potential therapeutic target in CESC, while highlighting the complex, isoform-specific roles of *LDH* family members in cervical cancer pathogenesis. Our results provide new insights into metabolic reprogramming in CESC and suggest *LDHC* may represent a novel protective factor in cervical carcinogenesis.

Keywords

LDH Family, Cervical Squamous Cell Carcinoma (CESC), Biomarker, DNA Methylation, Immune Infiltration, *LDHC*

1. Introduction

Cervical Squamous Cell Carcinoma (CESC), alongside breast, colorectal, and lung cancers, ranks among the four most prevalent malignancies in women [1]. CESC primarily manifests as two histological subtypes—squamous cell carcinoma and adenocarcinoma, with squamous cell carcinoma being more predominant, largely due to its association with human papillomavirus (HPV) infection [2]. Pathogens such as HPV [3], *Helicobacter pylori*, hepatitis B virus, and Epstein-Barr virus (EBV) contribute significantly to the rising morbidity and mortality of CESC. Clinical management strategies depend on tumor stage [4] and grade, with common interventions including radical hysterectomy [5] [6], brachytherapy [7], chemotherapy, immunotherapy [8], and combination therapies. Recent clinical trials have demonstrated that checkpoint inhibitors like ipilimumab and nivolumab synergistically modulate cervical tumor microenvironments, enhancing therapeutic efficacy [9]. However, due to the limited research on specific immune biomarkers for CESC and its persistently high mortality rate, identifying novel, highly sensitive, and specific tumor markers remains a critical research focus.

Tumor cells predominantly rely on glycolysis for energy supply, and excessive glycolytic activity has been established as a key driver of tumor progression [10]. Lactate dehydrogenase (*LDH*), a family of NAD+-dependent isoenzymes, catalyzes the interconversion of pyruvate and lactate while mediating the redox exchange between NADH and NAD+ [11]. This enzymatic activity underscores its pivotal role in the Warburg effect [12]. Notably, inhibition of lactate dehydrogenase A (*LDHA*) disrupts serine and aspartate biosynthesis, indirectly activating the GCN2-ATF4 signaling axis. This upregulates SLC1A5 expression and enhances glutamine/essential amino acid uptake, ultimately promoting mTORC1 activation and prolonging tumor cell survival [13]. Recently discovered *LDH* family members, lactate dehydrogenase A-like 6A (*LDHAL6A*) and 6B (*LDHAL6B*), are reportedly expressed exclusively in testicular tissue [14]. Additionally, antimetabolic agents have been shown to suppress CESC cell proliferation by targeting glycolysis-related proteins, such as lactate dehydrogenase B (*LDHB*) [15]. Lactate dehy-

drogenase C (*LDHC*), located on chromosome 7, was the first testis-specific isozyme identified in male germ cells [16]. Conversely, alterations in lactate dehydrogenase D (*LDHD*) expression influence lactate metabolism via glycolysis, with elevated *LDHD* levels observed in renal cell carcinoma [17] and esophageal squamous cell carcinoma [18] compared to normal tissues. Despite these findings, the roles of *LDHC* and *LDHD* in CESC pathogenesis remain poorly understood.

In this study, we comprehensively analyzed the expression profiles of *LDH* family members across human tissues and their differential expression patterns in pan-cancer. Utilizing multi-omics approaches, we investigated the *LDH* gene family's involvement in CESC and evaluated its diagnostic and prognostic potential through GEO dataset validation. Receiver operating characteristic (ROC) curve analysis further confirmed the robust diagnostic efficacy of most *LDH* members in CESC prognosis. Kaplan-Meier (KM) survival analysis revealed significant associations between *LDH* family expression and patient survival, supporting their utility as prognostic biomarkers. Additionally, we conducted mutation interaction, methylation correlation, and immune infiltration analyses, complemented by cellular validation experiments focusing on *LDHC*. This systematic exploration elucidates the functional relevance of *LDHC* and other *LDH* members in CESC progression, diagnosis, and clinical outcomes, providing a theoretical foundation for future diagnostic and therapeutic strategies targeting the *LDH* family in CESC.

2. Materials and Methods

2.1. Data Source and Processing

The expression profiles, prognostic significance, and immune cell infiltration patterns of *LDH* gene family members were analyzed using data from the TCGA database (https://portal.gdc.cancer.gov) [19], accessed via the Xiantao Academic platform (https://www.xiantaozi.com/login). Transcripts per million (TPM) normalized expression matrices were downloaded and log2-transformed (log2[value + 1]) for downstream analyses. To externally validate the diagnostic and prognostic relevance of *LDH* genes in CESC, we obtained the GSE63514 and GSE44001 datasets from the GEO database (https://www.ncbi.nlm.nih.gov/geo) and plotted receiver operating characteristic (ROC) curves. The area under the ROC curve (AUC) was calculated, and the closer the value was to 1, the higher the diagnostic efficiency. In the analysis, normal controls were pathologically confirmed normal tissues (paired adjacent or healthy donor), with cases being histologically diagnosed CESC samples. The diagnostic value of these genes is significant for $P < 0.05$.

2.2. mRNA Expression Analysis of the *LDH* Family

The Human Protein Atlas (HPA) database (https://www.proteinatlas.org) [20] was employed to evaluate *LDH* family expression across human tissues. Using the

"TISSUE" module and GTEx dataset, we queried the official gene symbols of *LDH* members (e.g., *LDHA*, *LDHB*) to generate tissue-specific expression profiles. Using the Xiantao Academic database, we selected three matched pairs of cervical cancer tumor tissues and adjacent normal tissues to compare *LDH* family gene expression profiles. The GSE63514 dataset was analyzed to confirm differential *LDH* expression in CESC versus normal cervical tissues. Diagnostic performance was assessed via receiver operating characteristic (ROC) curves using the "pROC" R package.

2.3. Protein Expression Levels of *LDH* Family Members

Immunohistochemical (IHC) staining results for *LDH* proteins in CESC and normal cervical tissues were retrieved from the HPA database using the "PATHOLOGY" and "TISSUE" modules. Clinical metadata for these samples were systematically curated to ensure relevance.

2.4. Prognostic Analysis of *LDH* Family Members

The Xiantao Academic database analyzed the association between *LDH* gene expression and three survival endpoints: Overall Survival (OS), Disease-Specific Survival (DSS) and Progress-Free Interval (PFI). Clinical and expression data from GSE44001 were processed via the Sangerbox platform (http://sangerbox.com/) as follows: Dataset and clinical metadata were retrieved using the "GSE44001" identifier. Probe annotation and data normalization were performed in the "Data Tabulation and Interactive Analysis" module. Survival analysis was conducted using the survival R package (v3.3.1), correlating *LDH* expression with CESC prognosis. Univariate and multivariate Cox regression models were applied to evaluate *LDH* genes as independent prognostic factors, implemented through the Xiantao Academic database.

2.5. Genetic Variation and Protein Interaction Networks of *LDH* Family Members

To investigate the mutational landscape of *LDH* family members in CESC, we utilized the cBioPortal database (https://www.cbioportal.org/) [21]. Protein-protein interaction (PPI) networks for *LDH* family members were constructed using the GeneMANIA database (http://genemania.org) [22] and STRING database (https://cn.string-db.org/) [23]. Subsequently, interacting genes were subjected to Kyoto Encyclopedia of Genes and Genomes (KEGG) and Gene Ontology (GO) enrichment analyses via the "ClusterProfiler" R package, with results visualized using ggplot2.

2.6. DNA Methylation Analysis of *LDH* Family

DNA methylation levels of *LDH* family members were analyzed using the UALCAN online database (https://ualcan.path.uab.edu/) [24] [25]. The GSCALite database (http://bioinfo.life.hust.edu.cn/web/GSCALite/) [26] was employed to as-

sess correlations between mRNA expression and DNA methylation, with results presented as scatter plots.

2.7. Correlation with Immune Cell Infiltration and Checkpoints

The Xiantao Academic Database (https://www.xiantaozi.com/login) was used to evaluate: Associations between *LDH* family gene expression and immune cell infiltration in CESC. Correlations between *LDH* members and immune checkpoint genes, including *PDCD1*, *CD274*, *PDCD1LG2*, *CTLA4*, *LMTK3*, *LAG3*, *TIGIT*, *HAVCR2* and *SIGLEC15.2*.

2.8. Single-Gene Enrichment Analysis of *LDHC*

Using the Researcher's Home database (https://www.home-for-researchers.com/#/), we explored *LDHC*-regulated signaling pathways in cervical cancer progression. CESC patients were stratified into high- and low-*LDHC* expression groups based on median expression values. Differentially expressed genes (DEGs) were identified using the "DESeq2" R package ($|\log2FC| \geq 1.5$, $*p* < 0.05$), followed by GO/KEGG enrichment analyses ("ClusterProfiler") and visualization.2.

2.9. Cell Culture

HeLa cells (ATCC) were cultured in DMEM high-glucose medium (Gibco, C11995500BT) supplemented with 10% FBS (Sigma, F8318) and 1% penicillin/streptomycin (Gibco, 15140122) at 37˚C with 5% CO_2. Cells in the logarithmic growth phase were harvested using trypsin (Gibco, 25200056) for experiments, with triplicate wells for all assays.

2.10. CCK-8 Assay

Cells (3,000/well) were seeded in 96-well plates (Corning, 3599) with 100 μL medium. Five plates were prepared to measure OD450 values at 0 h (post-attachment), 24 h, 48 h, 72 h, and 96 h. Before measurement, CCK-8 reagent (UElandy, C6005M) was diluted (10% medium: CCK-8 = 1:9), and 10 μL was added to each well. After 1-hour incubation, absorbance was measured using a VICTOR Nivo plate reader, and proliferation curves were plotted.

2.11. Colony Formation Assay

Log-phase cells (3,000/well) were seeded in 6-well plates (Corning, 3516) and cultured for 14 days (medium replaced every 2 - 3 days). When clusters reached 30 - 50 cells/field, cultures were terminated. Cells were: 1) Washed with PBS (Gibco, C10010500). 2) Fixed with 4% paraformaldehyde (biosharp, BL539A) for 30 min. 3) Stained with crystal violet (Solarbio, G1063) for 40 min. 4) Imaged, and colonies (>50 cells) were counted.

2.12. Wound Healing Assay

Cells were seeded in 6-well plates at a density of 2×10^5 cells/mL and incubated

until reaching approximately 90% confluence. A uniform scratch was created using a sterile pipette tip perpendicular to the plate bottom. Initial wound area (0 h) was measured using an inverted microscope (Axio Vert A1, 07060200) by capturing multiple fields. After 48 h incubation, the same fields were re-imaged to measure remaining wound area. The migration rate was calculated as: Scratch healing rate (%) = [(0 h area − 48 h area)/0 h area] × 100ys.

2.13. Cell Invasion and Migration Assays

Transwell chambers (JET, TCS003024) were used for both assays. For invasion experiments, 100 μL Matrigel (Corning, 356234) was evenly coated and polymerized in the upper chamber. Cells (2×10^5 cells/mL in serum-free medium) were seeded in the upper chamber, while 10% FBS medium served as chemoattractant in the lower chamber. After 24 h incubation, non-migrated cells were removed with PBS. Migrated/invaded cells were fixed with 4% paraformaldehyde (50 min), stained with 0.1% crystal violet (50 min), and counted from four random microscope fields per chamber.

2.14. Western Blotting

Total protein was extracted using RIPA lysis buffer (Aase, PC103) supplemented with 1% PMSF (Aase, GRF101). Protein concentration was determined (Aase, ZJ102) and normalized. Samples were separated on 7.5% SDS-PAGE gels (Aase, PG211) at 80 V (40 min) then 120 V (35 min), followed by transfer to methanol-activated PVDF membranes (Millipore, IPVH00010) at 200 mA for 60 min. Membranes were blocked (Yase, PS108P, 40 min), incubated with primary antibodies (Proteintech *LDHC*: 19989-1-AP, 4˚C overnight) and HRP-conjugated secondary antibodies (Invitrogen 31460/31430, 2 h RT). Protein bands were visualized using ECL reagent (Accelerase, SQ201) and quantified with ImageJ.

2.15. Quantitative RT-PCR

Total RNA was extracted using TRIzol (Yingjie Life, 15596026) and reverse transcribed (Tolobio, 22107). qPCR was performed with SYBR Green (Tolobio, 22204-1) under conditions: 94˚C (3 min); 35 cycles of 94˚C (15 s), 64˚C (2 min), 72˚C (2 min); final extension at 72˚C (10 min). Relative expression was calculated via $2^{(-\Delta\Delta Ct)}$ method. Primer sequences are listed in Table 1.

Table 1. Primer sequences used as target and reference genes used in qPCR reactions.

Gene name	Primers	Sequence
LDHA	forward primer	CGGATCTCATTGCCACGC
	reverse primer	CACCAACCCCAACAACTGTA
LDHAL6A	forward primer	CTTGTCCTTGTGGATGTTGATG
	reverse primer	TCTCCTTTTTTCTGGCGTGC

Continued

LDHAL6B	forward primer	GAGTTGGACTGTGCCTGTTG
	reverse primer	ATCTTGCTCACGGGGGT
LDHB	forward primer	GACTTTGTCTTCTCCGCACGA
	reverse primer	GCTGATAGCACACGCCATACC
LDHC	forward primer	GCCATAACGACGCATACTAAAAG
	reverse primer	GCCATAACGACGCATACTAAAAG
LDHD	forward primer	CAACCTCACGGGGCTCTTCG
	reverse primer	AACTCAATGCGGGCTACGGG
GAPDH	forward primer	CCTGGGAAACCTGCCAAGTATG
	reverse primer	GGTCCTCAGTGTAGCCCAAGATG

2.16. Statistical Analysis

The Mann-Whitney U test was used to analyze the expression levels of unpaired samples of *LDH* family in pan-cancer, and the Wilcoxon singed rank test was used to process the paired samples. The prognostic survival analysis of *LDH* family in pan-cancer was performed by one-way and multifactorial Cox regression test as the statistical analysis of variance. Immunocorrelation analysis using Spearman correlation coefficient was used to determine the relationship between two variables. Experimental data were taken as mean ± standard deviation after three independent experiments, and paired samples were statistically analyzed using the paired t-test, with $p \leq 0.05$ considered statistically significant.

3. Results

3.1. Tissue-Specific Expression of *LDH* Family Members

The study design is illustrated in Figure 1. Analysis of the Human Protein Atlas (HPA) database revealed distinct tissue distribution patterns for *LDH* family members (Figure 1). *LDHA* demonstrated predominant expression in retina, liver, and skeletal muscle, while *LDHB* showed significantly higher expression in midbrain, kidney, and cardiac muscle—tissues with high aerobic metabolic activity. Consistent with previous reports, both *LDHAL6B* and *LDHC* exhibited exclusive testicular distribution. *LDHD* was primarily expressed in liver, cardiac muscle, and skeletal muscle. These findings collectively demonstrate that *LDH* family members display tissue-specific expression patterns, with particular enrichment in organs exhibiting high oxygen consumption.

3.2. Pan-Cancer mRNA Expression Profiling

Our comprehensive analysis revealed cancer-type specific expression patterns for each *LDH* family member (Figure 2). *LDHA* was significantly upregulated in 14

cancer types including BRCA, CESC, and GBM, while being downregulated in KICH (Figure 2(A)). *LDHAL6A* showed elevated expression in CHOL, LIHC and STAD tumors compared to 11 other cancer types where its expression was reduced (Figure 2(B)). *LDHAL6B* expression was increased in GBM, HNSC, KIRC and STAD tumor tissues relative to their normal counterparts (Figure 2(C)). *LDHB* exhibited upregulation in 8 cancer types including CHOL and LIHC, but downregulation in 6 others (Figure 2(D)). *LDHC* was overexpressed in CESC, ESCA and HNSC tumors while being underexpressed in 5 cancer types (Figure 2(E)). Notably, *LDHD* showed tumor-specific expression limited to KICH and LUAD, despite being widely expressed in normal tissues (Figure 2(F)).

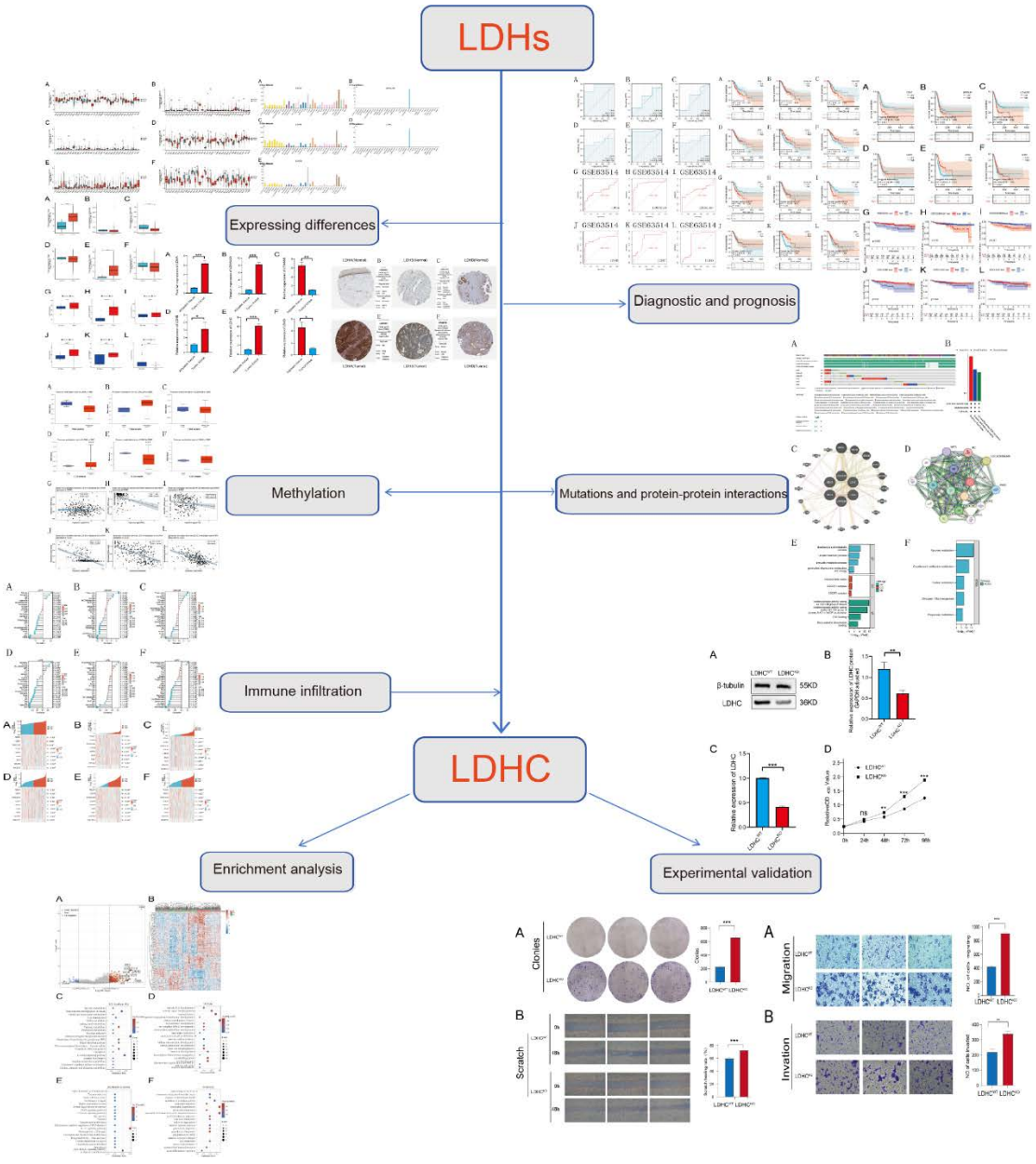

Figure 1. General flow chart of the article.

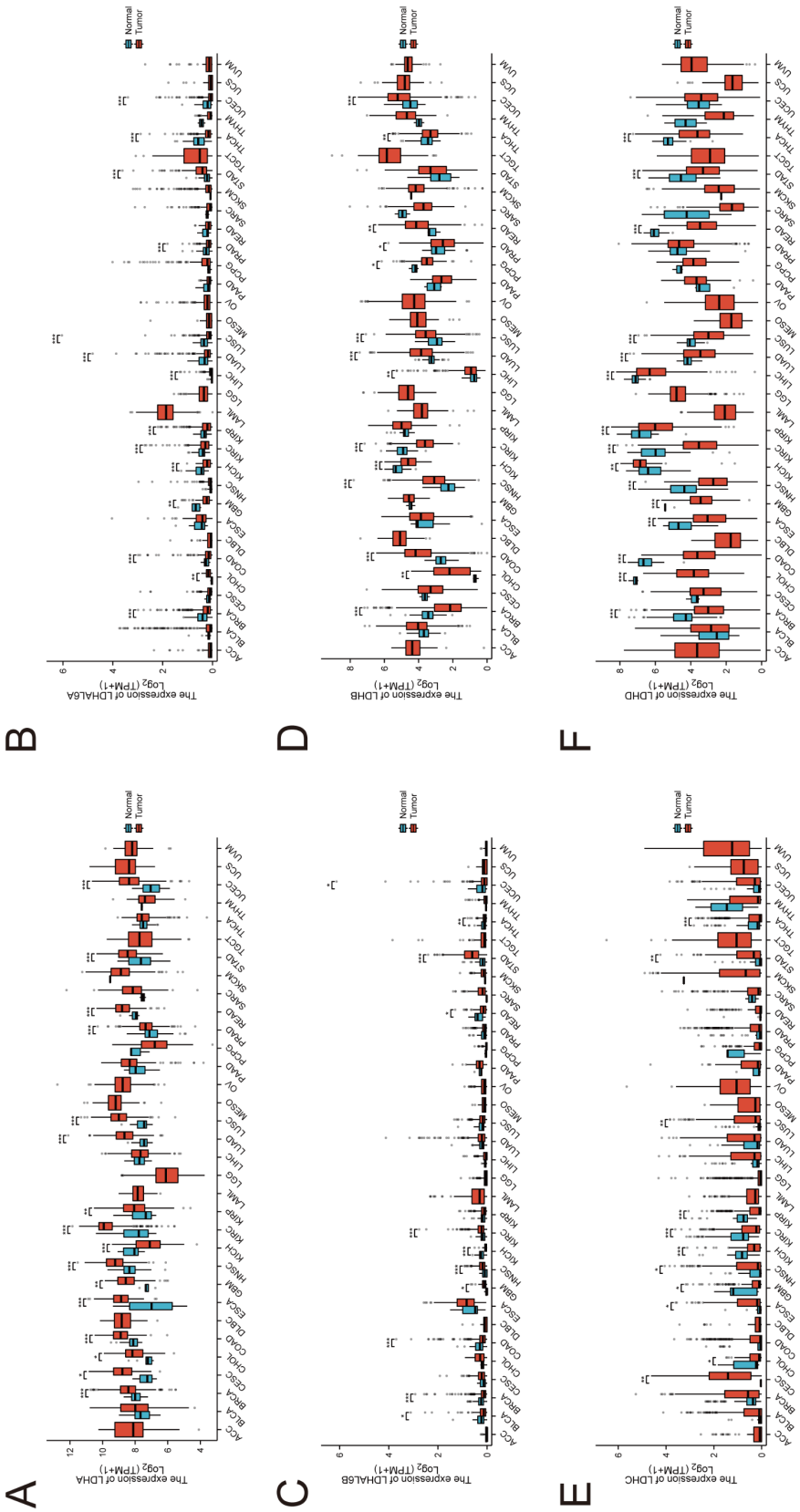

Figure 2. Expression analysis of *LDH* family in pan-cancer. (A) *LDHA*; (B) *LDHAL6A*; (C) *LDHAL6B*; (D) *LDHB*; (E) *LDHC*; (F) *LDHD*.

3.3. Differential Expression in Cervical Cancer

Comparative analysis between CESC and adjacent normal tissues yielded important findings (Figure 3). TCGA data revealed significant upregulation of *LDHA* and *LDHC* in tumor tissues, while *LDHAL6B* showed higher expression in normal tissue (Figure 3(A)-(F)). External validation using GSE63514 dataset confirmed increased expression of *LDHAL6A*, *LDHB* and *LDHC* in tumors, with *LDHD* being more highly expressed in normal cervical tissue (Figure 3(G)-(L)). PCR validation of clinical samples largely corroborated these findings, showing predominant tumor overexpression of most *LDH* members except for *LDHAL6B* and *LDHD* (Figure 3(A)-(F)).

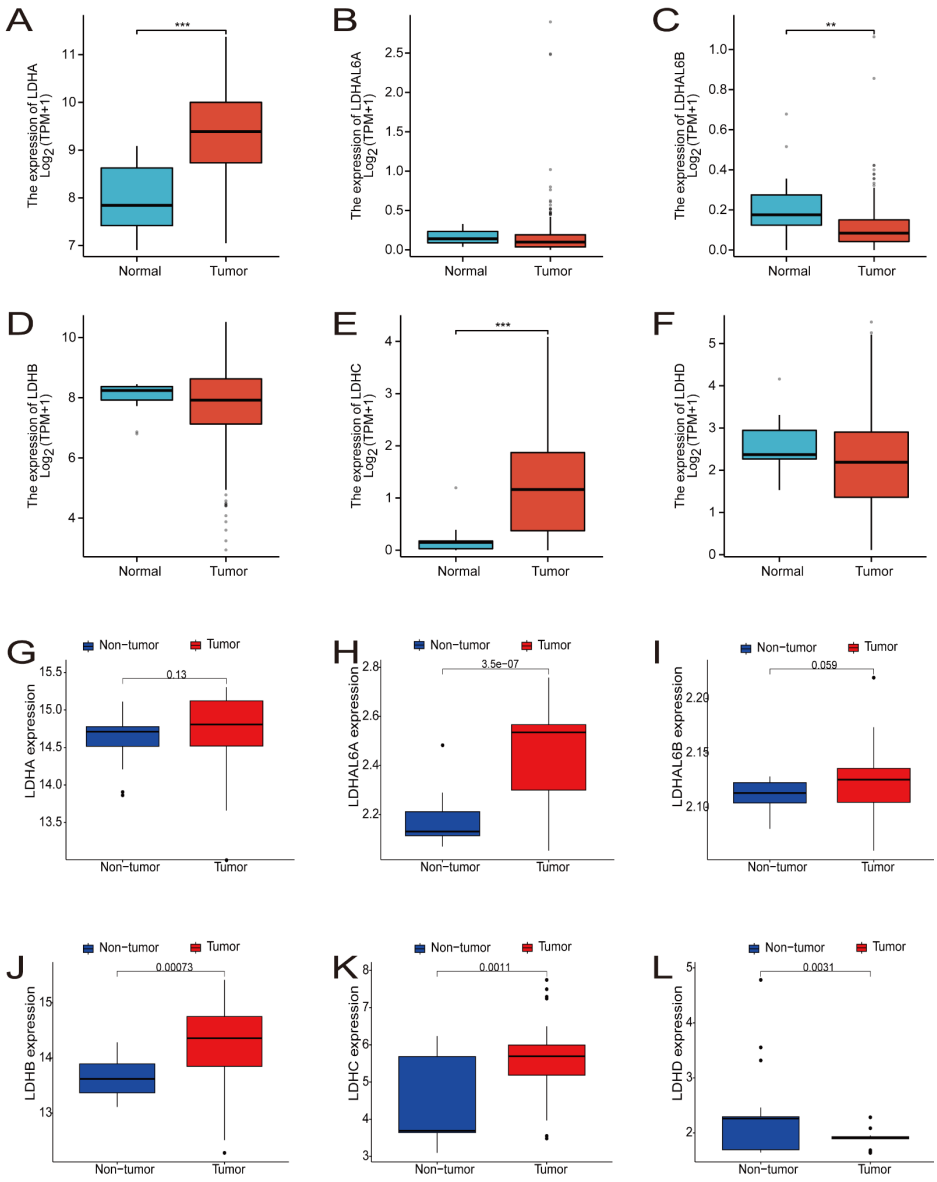

Figure 3. Expression analysis of *LDH* gene family in cervical cancer. (A) - (F) Differential expression of *LDH* gene family members in the TCGA database. (G) - (L) Differential expression of *LDH* family members in the external validation GES63514.3.4. Some Common Mistakes.

3.4. Diagnostic Potential in CESC

ROC curve analysis demonstrated the diagnostic value of *LDH* family members in CESC. TCGA data revealed exceptional diagnostic performance for *LDHC* (AUC = 0.950, 95% CI: 0.921 - 0.980) and *LDHA* (AUC = 0.915, 95% CI: 0.766 - 1.000), with other members showing moderate diagnostic value (**Figure 4(A)-(F)**). The GSE63514 validation cohort confirmed *LDHC*'s strong diagnostic potential (AUC = 0.884) (**Figure 4(G)-(L)**). These consistent results across independent datasets highlight *LDHC* as the most promising diagnostic biomarker among *LDH* family members for cervical cancer.

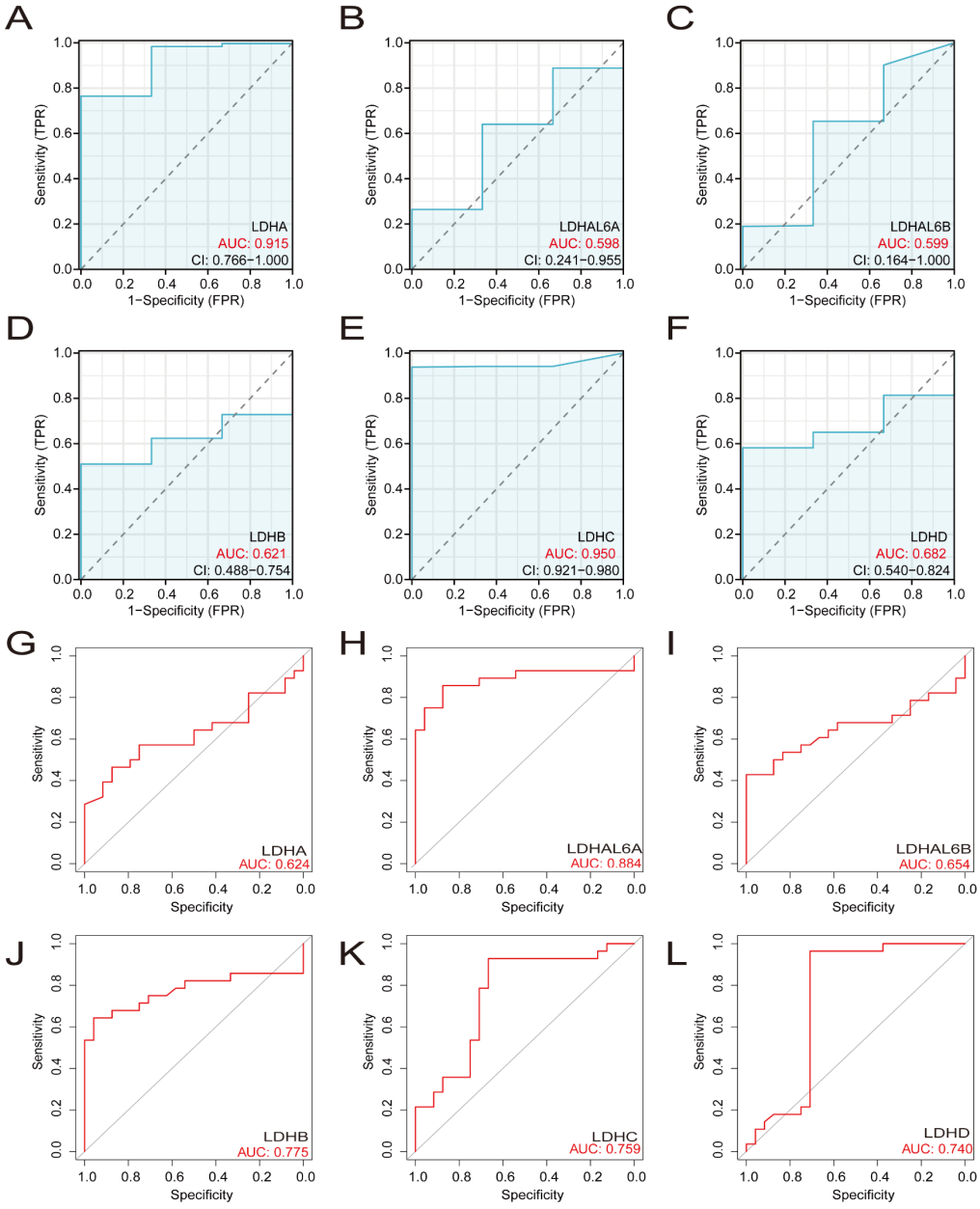

Figure 4. Diagnostic efficacy of *LDH* gene family in cervical cancer. (A) - (F) Diagnostic efficacy of *LDH* gene families in the TCGA database. (G) - (L) Diagnostic efficacy of *LDH* gene family members in the external validation dataset GES63514.

3.5. Protein Expression Validation

Immunohistochemical analysis from the HPA database provided protein-level confirmation of our findings. *LDHA*, *LDHB* and *LDHD* all showed significantly higher protein expression in CESC compared to normal cervical tissues (Figure 5(A)-(F)). The remaining three *LDH* family members were not detectable in the database, suggesting potential tissue-specific expression limitations.

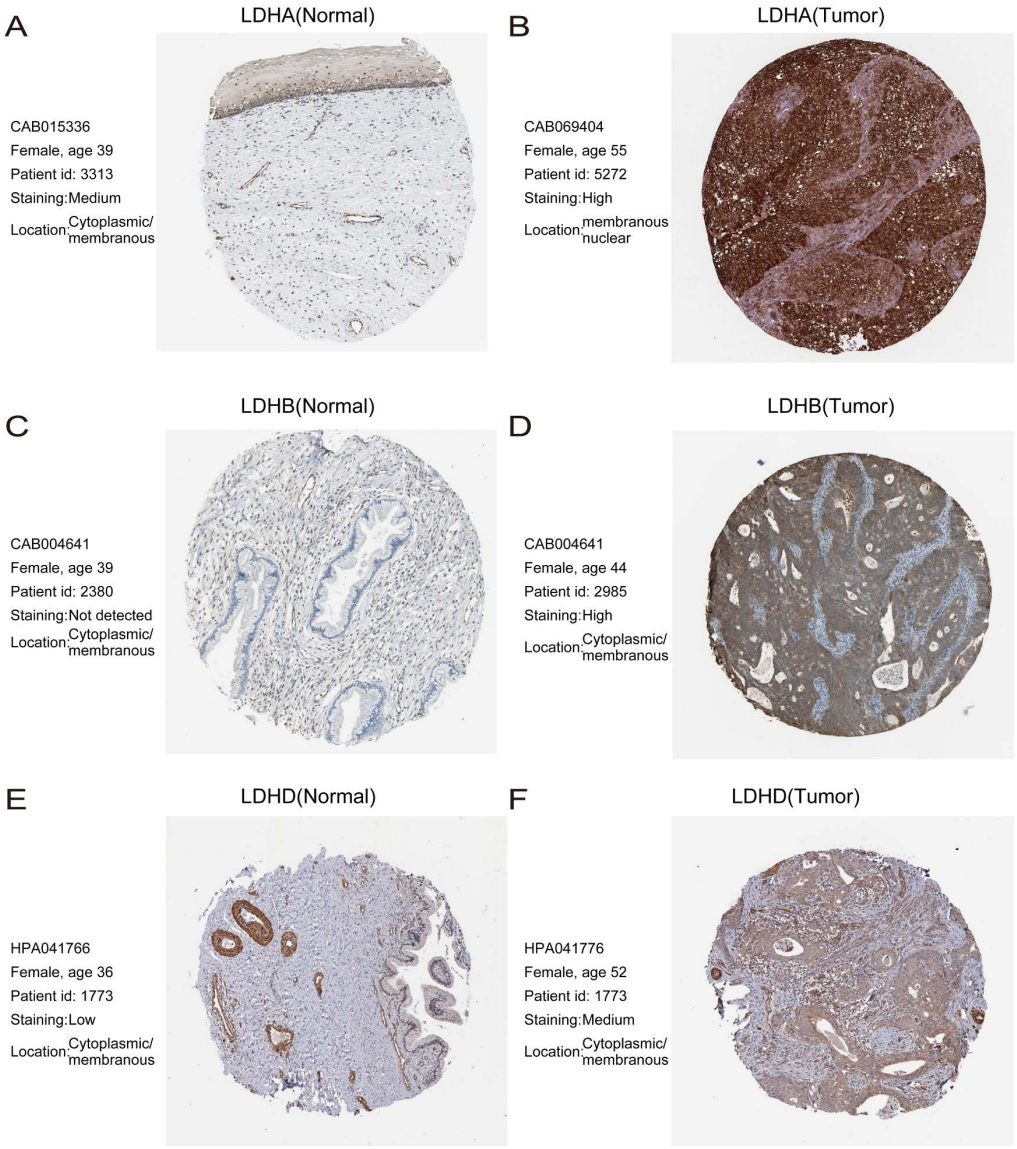

Figure 5. Protein levels of *LDH* family in cervical cancer. (A) - (B) Protein expression levels of *LDHA* in normal cervical tissues and cervical cancer tissues, respectively; (C) - (D) Protein expression of *LDHB* in normal cervical tissues and cervical cancer, respectively.

3.6. Prognostic Significance in CESC

Survival analysis revealed important clinical correlations (Figure 6). High expression of *LDHA* and *LDHAL6B* was associated with worse overall survival (OS), while elevated *LDHB*, *LDHC* and *LDHD* correlated with better outcomes (Figure 6(A)-

(F)). Similar trends were observed for disease-specific survival (DSS) and progression-free interval (PFI), with *LDHC*-high patients showing particularly favorable prognosis (Figure 6(G)-(L), Supplementary Figure 4(A)-(F)). External validation using GSE44001 dataset confirmed the adverse prognostic association of *LDHA*, *LDHAL6A* and *LDHAL6B* high expression (Supplementary Figure 4(G)-(L)).

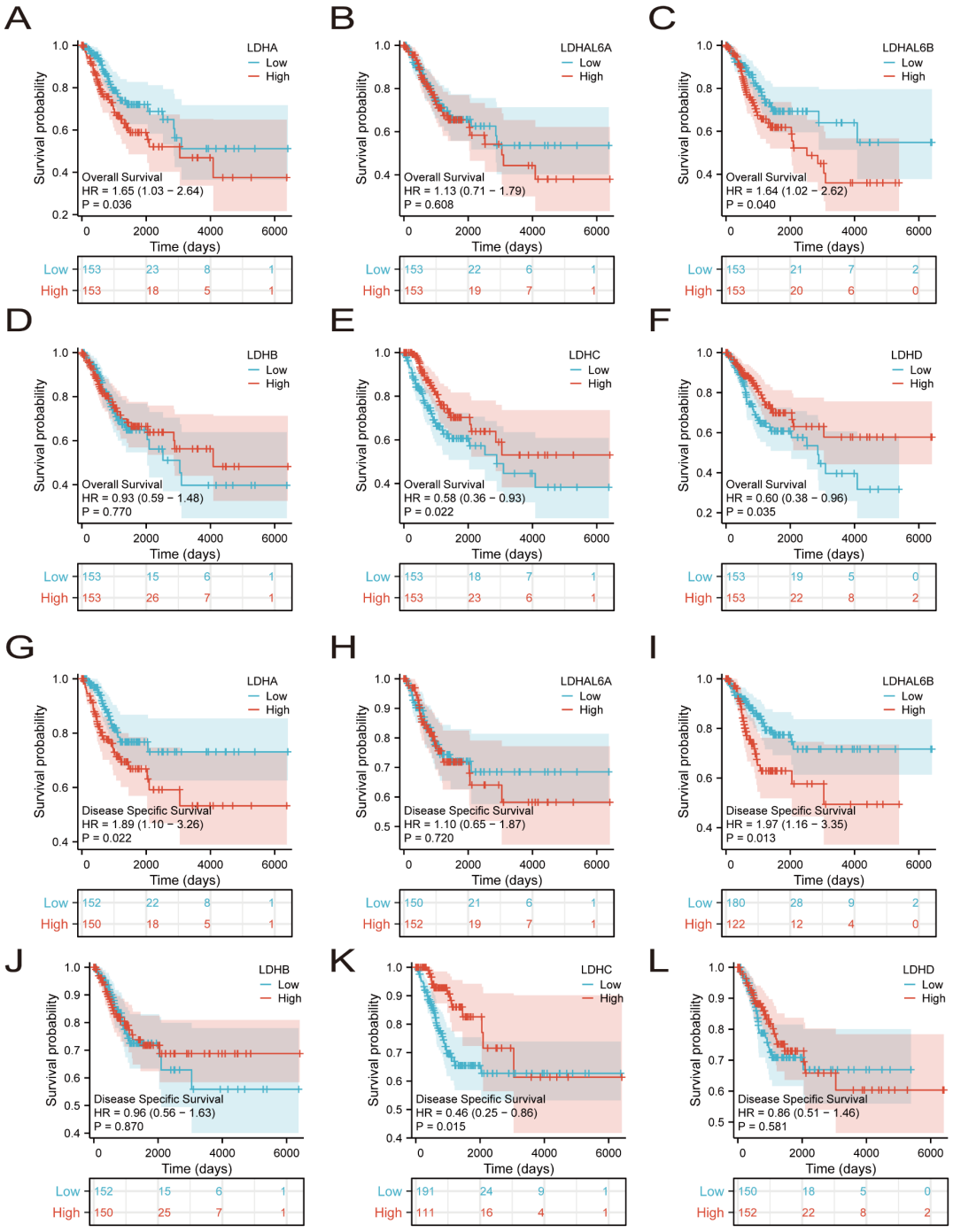

Figure 6. Effect of *LDH* gene family on survival of cervical cancer patients. (A) - (F) Effect of *LDH* gene family members in the TCGA database on overall survival (OS) of cervical cancer patients. (G) - (L) Effect of *LDH* gene family members in the TCGA database on disease-specific survival (DSS) in cervical cancer patients.

Cox regression analysis identified four genes (*LDHA*, *LDHAL6B*, *LDHC*, *LDHD*) as significant prognostic factors in univariate analysis. Multivariate analysis further established *LDHAL6B* as an independent prognostic marker for CESC patients.

3.7. Mutation and Protein Interaction Networks of *LDH* Family Members

Comprehensive analysis of mutation patterns in CESC using the cBioPortal database revealed distinct mutation frequencies among *LDH* family members: *LDHA* (0.9%), *LDHAL6A* (0.8%), *LDHAL6B* (1%), *LDHB* (2.2%), *LDHC* (1.1%), and *LDHD* (1.5%), with gene amplification being the predominant mutation type (**Figure 7(A)-(B)**). Protein-protein interaction (PPI) networks constructed through GeneMANIA and STRING databases demonstrated extensive functional associations between *LDH* members and other proteins (**Figure 7(C)-(D)**). Subsequent functional enrichment analysis revealed that interacting proteins were primarily involved in critical metabolic processes including dicarboxylic acid metabolism, lactate metabolism, pyruvate metabolism, and energy production (**Figure 7(E)**). KEGG pathway analysis further identified significant enrichment in pyruvate metabolism, cysteine and methionine metabolism, carbon metabolism, glycolysis/gluconeogenesis, and propanoate metabolism (**Figure 7(F)**), highlighting the central role of *LDH* family members in cellular metabolic regulation.

3.8. DNA Methylation Patterns of *LDH* Family Members

Methylation analysis using UALCAN database demonstrated significant epigenetic differences between CESC and normal cervical tissues (**Figure 8(A)-(F)**). Notably, *LDHB* exhibited significantly higher methylation levels in tumor tissues, while *LDHC* showed marked hypomethylation. Correlation analysis between mRNA expression and methylation status revealed a significant negative association for *LDHAL6A*, *LDHAL6B*, *LDHB*, *LDHC*, and *LDHD* (**Figure 8(G)-(L)**), suggesting potential epigenetic regulation of these genes in cervical carcinogenesis. No significant correlation was observed between *LDHA* expression and methylation status.

3.9. Immune Microenvironment Associations of *LDH* Family Members

Comprehensive immune correlation analysis revealed distinct patterns of association between *LDH* family expression and immune cell infiltration (**Figure 9**). *LDHA* expression showed positive correlation with Th2 cells and neutrophils, while demonstrating negative associations with multiple immune cell types including eosinophils, Tregs, and dendritic cells. *LDHAL6A* exhibited positive correlations with Thelper cells and Tcm, while *LDHAL6B* showed associations with Thelper cells and neutrophils. Particularly noteworthy was *LDHC*'s exclusive positive correlation with NK CD56bright cells and negative association with TFH cells and macrophages. Immune checkpoint analysis demonstrated significant correlations between *LDH* members and key checkpoint molecules (Supplementary **Figure 2(A)-(F)**), with *LDHD* showing the most extensive interaction profile,

including positive correlation with *LMTK3* and negative associations with multiple checkpoints (*CD274*, *PDCD1LG2*, *CTLA4*, *LAG3*, and *HAVCR2*).

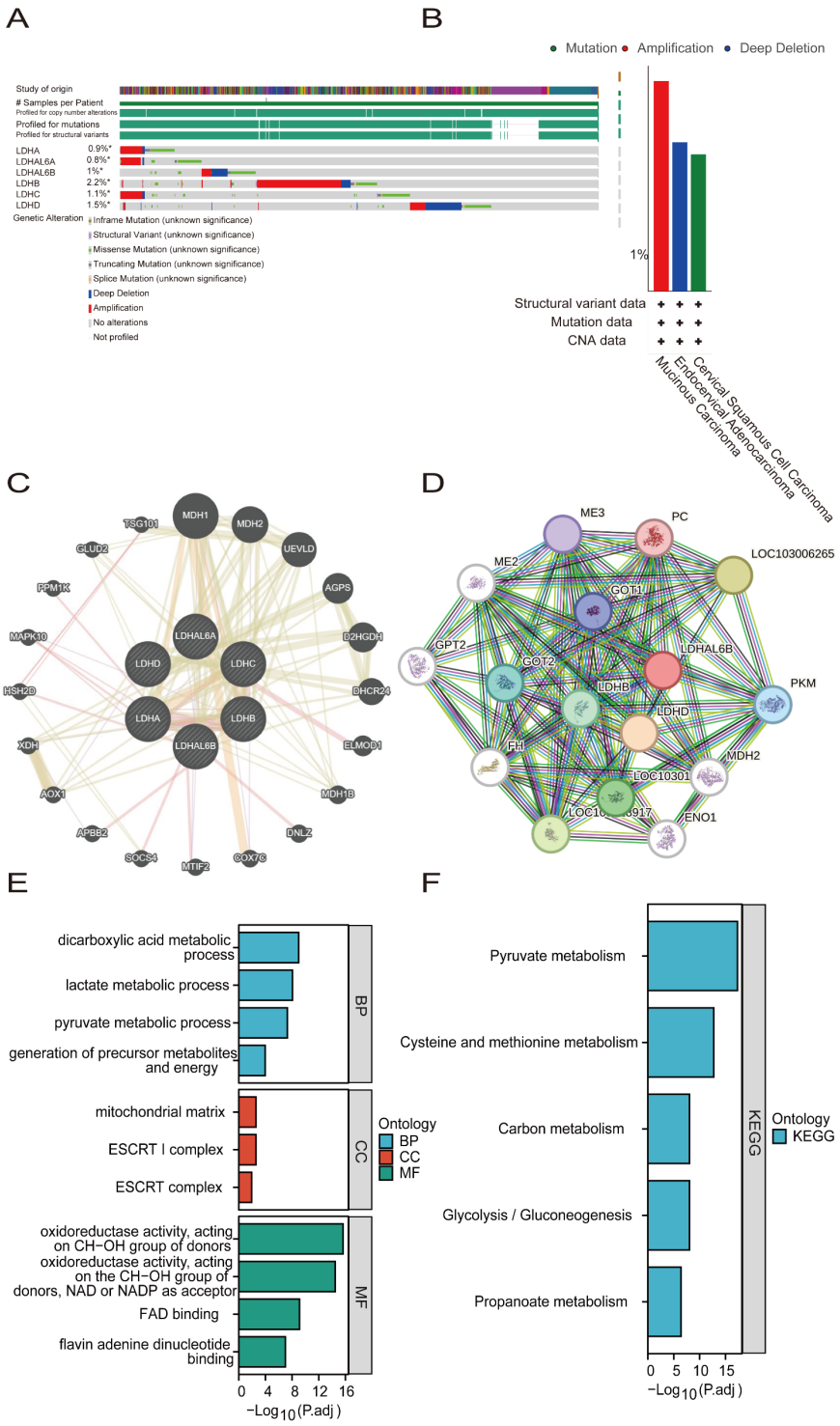

Figure 7. Mutational features of *LDH* gene family members and protein interactions network. (A) - (B) Mutational features of *LDH* family member genes in cervical cancer were described using the cBioPortal database; (C) construction of *LDH* gene family member interactions networks based on the Gene MANIA database; (D) analysis of protein interactions networks of *LDH* family members based on the STRING database; (E) - (F) GO and KEGG enrichment analysis.

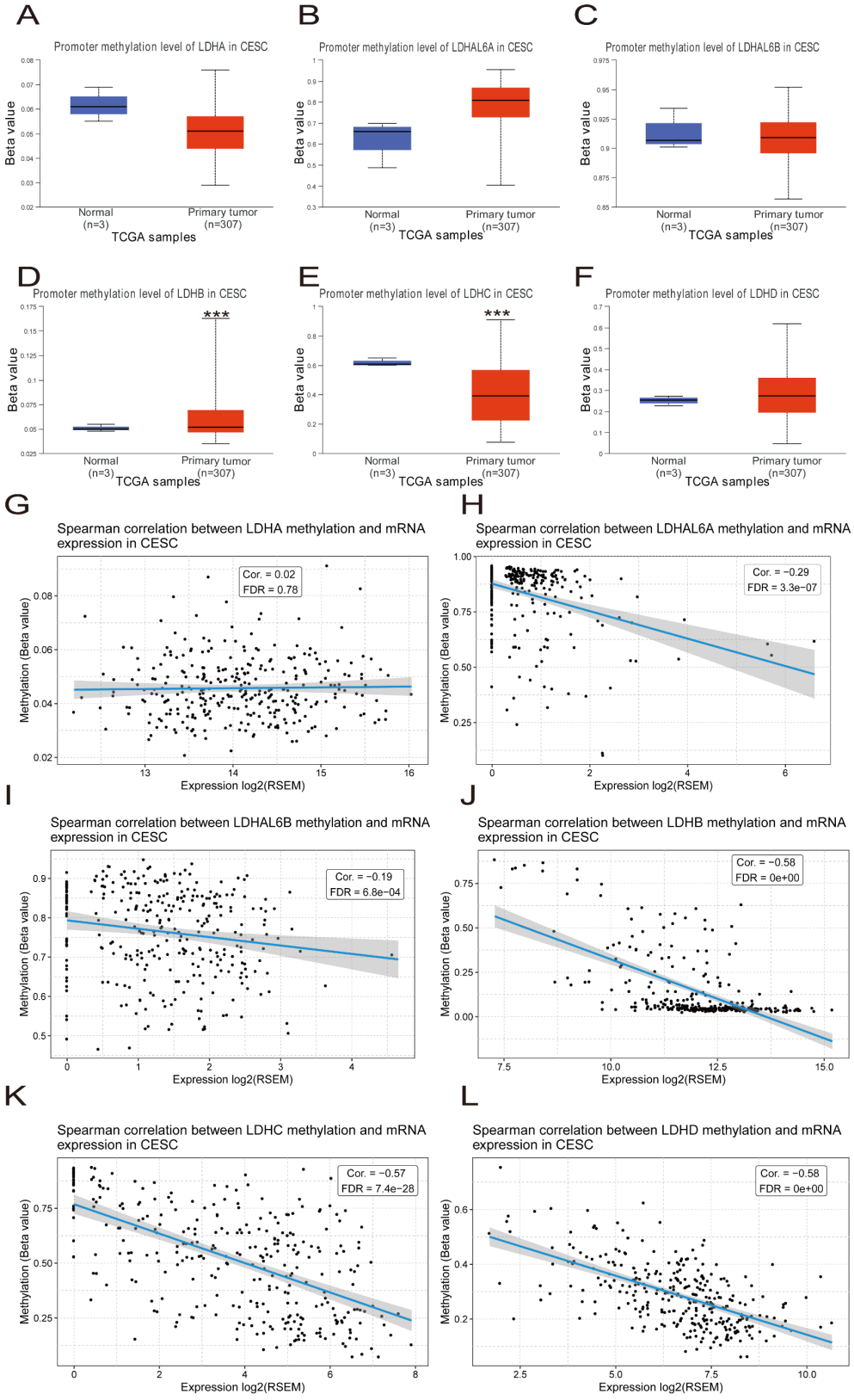

Figure 8. Methylation analysis of *LDH* gene family members. (A) - (F) Analysis of methylation level differences between *LDH* gene family members in cervical cancer tissues and paracellular carcinomas based on the UALCAN database; (G) - (L) Correlation between gene expression and methylation levels of *LDH* gene family members analyzed using MethSurv database.

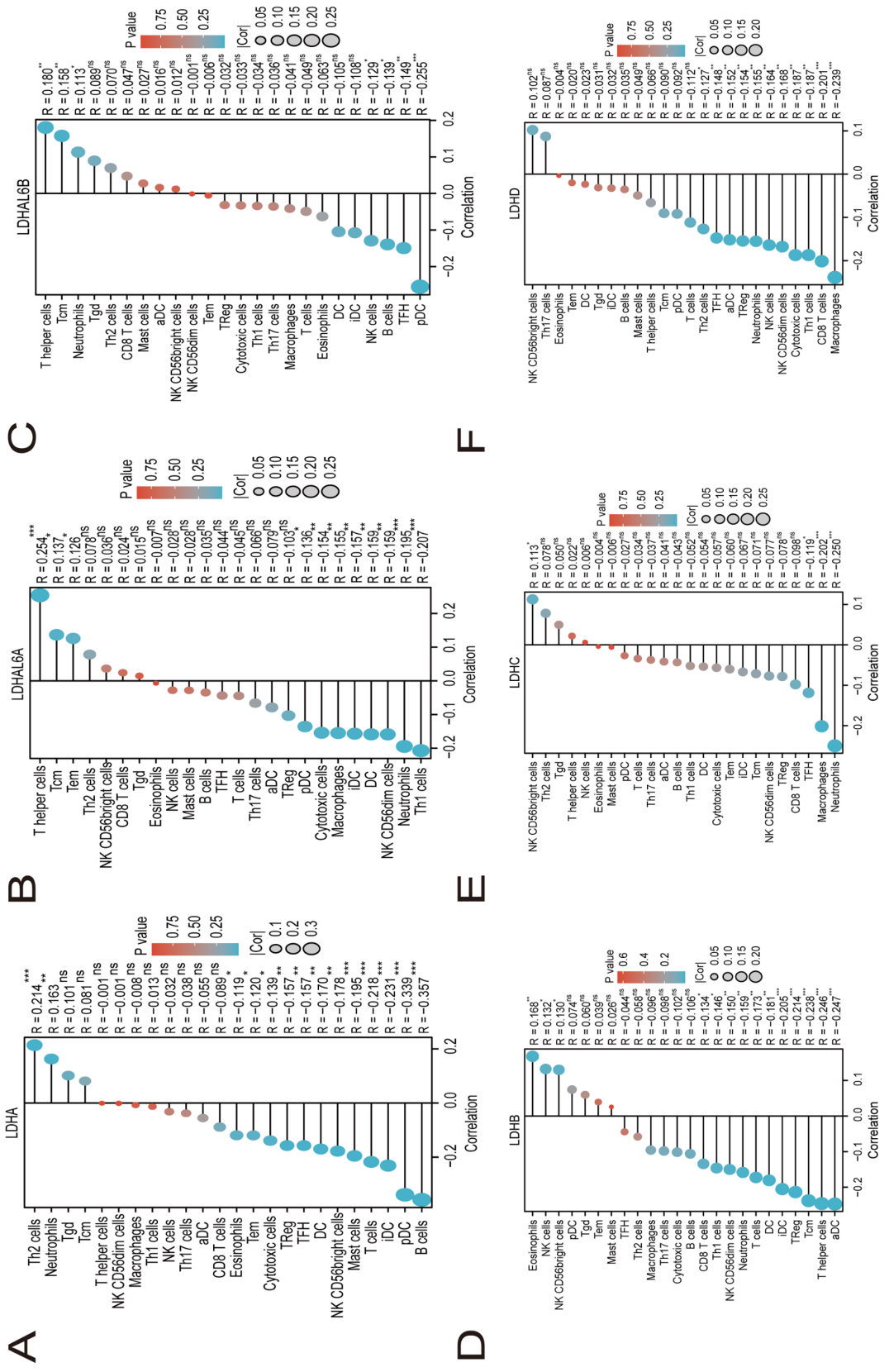

Figure 9. Correlation analysis of *LDH* gene family members with the level of immune cell infiltration in cervical cancer patients. (A) *LDHA*; (B) *LDHAL6A*; (C) *LDHAL6B*; (D) *LDHB*; (E) *LDHC*; (F) *LDHD*.

3.10. Functional Enrichment Analysis of *LDHC* in CESC

To elucidate *LDHC*'s functional role in CESC progression, we performed single-gene enrichment analysis after stratifying patients into high-(G1) and low-expression (G2) groups based on median *LDHC* expression. Differential expression analysis identified 264 significantly altered genes (226 upregulated, 38 downregulated) between the groups (**Figure 10(A)-(B)**). KEGG pathway analysis of upregulated genes revealed enrichment in tyrosine metabolism, transcriptional misregulation in cancer, and sulfur metabolism pathways (**Figure 10(C)**), while GO analysis highlighted involvement in developmental processes including ureteric bud development and sensory organ morphogenesis (**Figure 10(D)**). Downregulated genes were significantly enriched in pathways including α-linolenic acid metabolism and small cell lung cancer (**Figure 10(E)**), with GO terms related to immune regulation such as neutrophil migration and degranulation. These findings suggest *LDHC* may play multifaceted roles in both metabolic reprogramming and immune modulation during cervical cancer progression.

3.11. Validation of *LDH* Gene Family Expression and Functional Characterization of *LDHC* in CESC

To validate the expression patterns of *LDH* family members in cervical cancer, we analyzed clinical CESC specimens and adjacent normal tissues. Our results demonstrated significant upregulation of *LDHA, LDHAL6A, LDHB* and *LDHC* in tumor tissues, while *LDHAL6B* and *LDHD* showed marked downregulation (**Figure 3**). Given *LDHC*'s prominent diagnostic and prognostic value in CESC revealed by our preliminary analyses, coupled with the absence of prior functional studies, we selected this gene for further investigation using the Hela cell line. Successful knockdown of *LDHC* was confirmed at both transcriptional (qPCR) and translational (Western blot) levels (**Figure 11(A)-(C)**). Functional assays revealed that *LDHC* depletion significantly enhanced the malignant phenotype of CESC cells. CCK-8 proliferation assays showed accelerated growth kinetics in *LDHC*-knockdown cells (**Figure 11(D)**). This pro-tumorigenic effect was further supported by colony formation assays demonstrating increased proliferative capacity (**Figure 12(A)**), wound healing assays revealing enhanced migratory potential (**Figure 12(B)**), and Transwell experiments confirming greater invasive capability (**Figure 13(A)-(B)**). Collectively, these findings position *LDHC* as a potential tumor suppressor in cervical carcinogenesis.

4. Discussion

Our study provides the first comprehensive characterization of *LDH* family members in CESC, addressing a critical knowledge gap in the field. Through systematic analysis of expression patterns across normal and malignant tissues, we have identified distinct tissue-specific distributions: while *LDHA*, *LDHB* and *LDHD* exhibit ubiquitous expression, *LDHAL6B* and *LDHC* demonstrate testis-specific localization, consistent with their classification as testicular lactate dehydrogenase

isoforms [27] [28]. Notably, pan-cancer analysis revealed consistent overexpression of multiple *LDH* members in CESC and other malignancies, suggesting their potential as diagnostic biomarkers.

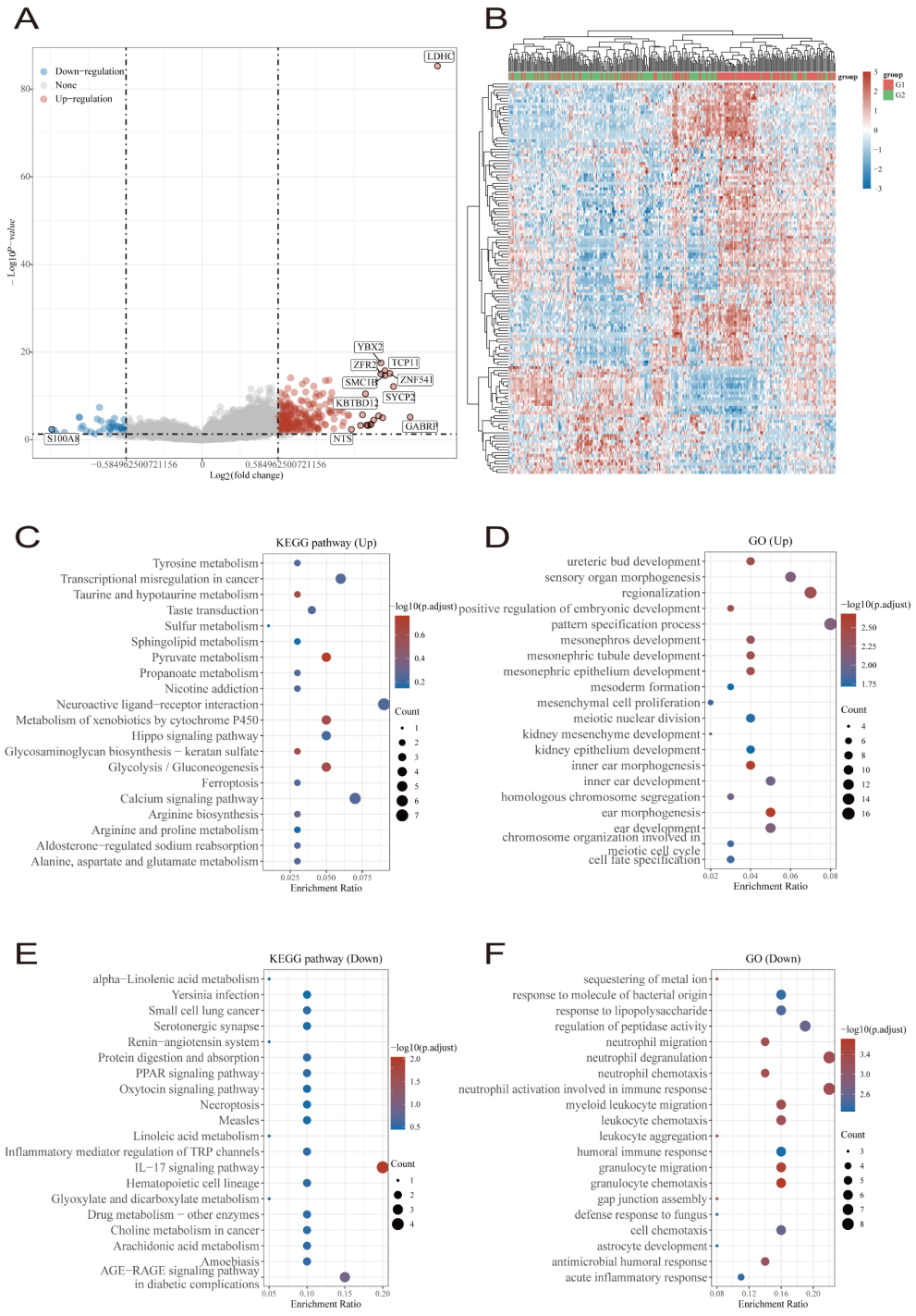

Figure 10. Single-gene pathway enrichment analysis of *LDHC*. (A) Differentially expressed genes (DEGs) in the *LDHC* high and low expression groups demonstrated by volcano plots; (B) Expression levels of *LDHC* high and low groups demonstrated by heatmaps; (C) KEGG pathway enrichment analysis of up-regulated genes; (D) GO pathway enrichment analysis of up-regulated genes; (E) KEGG pathway enrichment analysis of down-regulated genes; (F) GO pathway enrichment analysis of down-regulated genes.

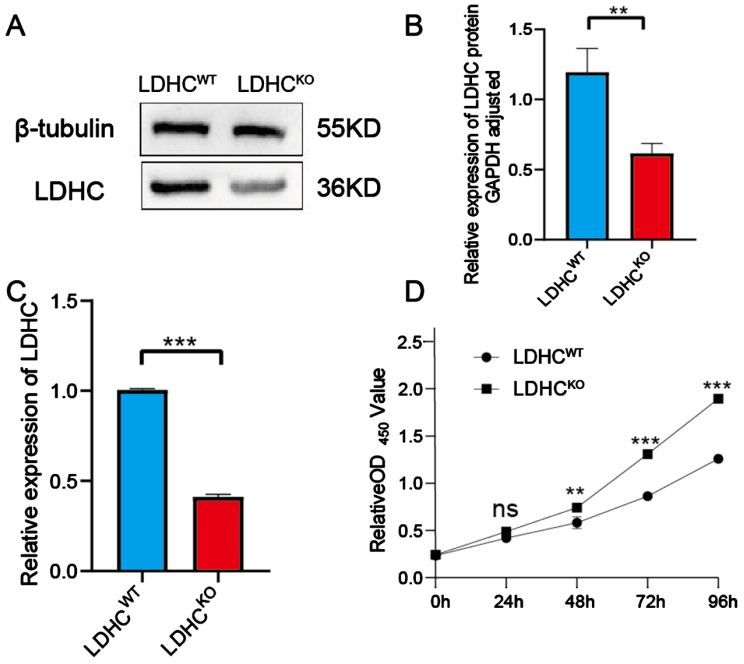

Figure 11. Construction of *LDHC* knockdown cell lines and the effect of *LDHC* knockdown on the proliferative ability of cervical cancer cells. (A) Verification of protein expression level differences between *LDHC* knockdown cell groups and wild cell lines by WB assay; (B) Quantitative analysis of protein levels after *LDHC* knockdown; (C) Verification of mRNA expression level changes after *LDHC* knockdown by RT-qPCR assay; (D) CCK8 proliferation assay of Cell.

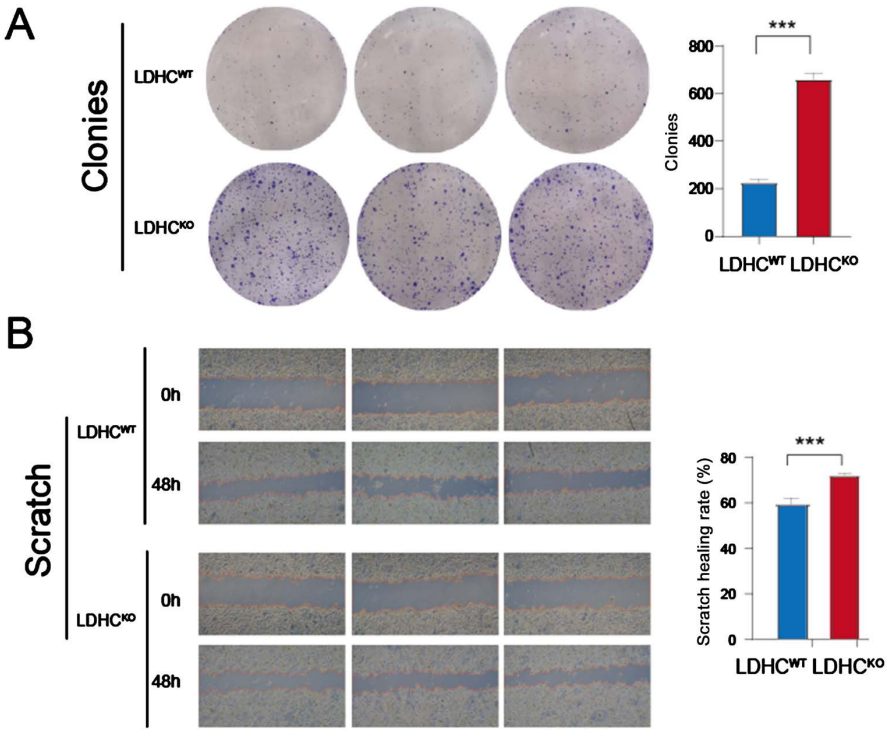

Figure 12. Effect of *LDHC* knockdown on proliferation and healing ability of cervical cancer cells. (A) cell clone formation experiment; (B) cell scratch healing experiment.

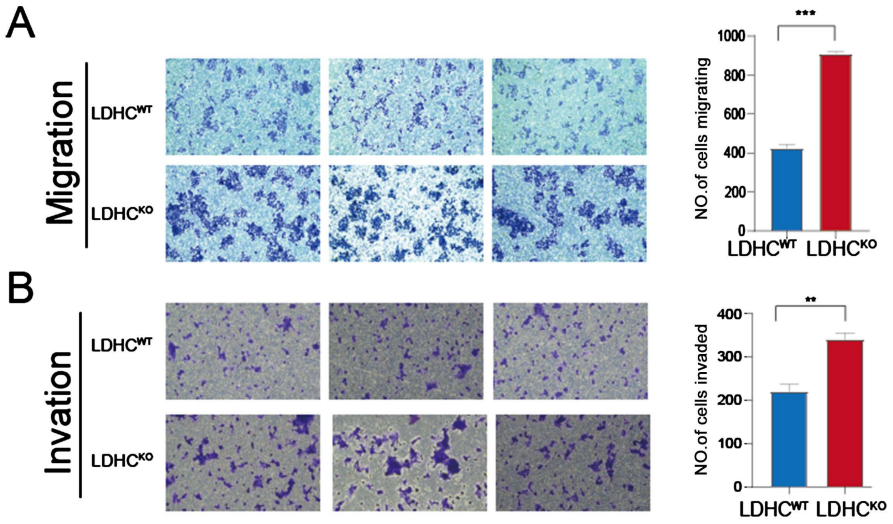

Figure 13. Effect of *LDH* knockdown on the migration and invasion ability of cervical cancer cells. (A) cell migration assay; (B) cell invasion assay.

The prognostic significance of *LDH* family members in CESC appears complex. While most members (*LDHA*, *LDHB*) correlate with poor outcomes when overexpressed, potentially through mechanisms like JNK-mediated apoptosis [29] or cis-platin resistance [15], *LDHC* presents a striking exception. *LDHC* demonstrates marked tissue-specific expression, suggesting its potential involvement in cervical carcinogenesis through distinct molecular regulatory mechanisms. Our clinical da-ta associate high *LDHC* expression with improved survival, a finding corroborated by functional studies showing that *LDHC* knockdown enhances proliferation, migration and invasion in Hela cells. Furthermore, our immune infiltration analysis revealed specific correlations between *LDHC* and antitumor immune cells, particularly NK CD56bright cells. This tumor-suppressive role contrasts with the onco-genic functions reported for other *LDH* isoforms and warrants further investigation to elucidate the underlying molecular mechanisms.

These findings have important implications for understanding cervical cancer pathogenesis and developing targeted therapies. The differential effects of *LDH* family members suggest that therapeutic strategies may need to be isoform-specific, particularly given *LDHC*'s unique protective role. Future studies should explore whether *LDHC*'s antitumor effects involve metabolic reprogramming or interactions with specific signaling pathways in cervical epithelial cells.

Our comprehensive mutation analysis revealed that *LDH* family members exhibit high mutation frequencies across various cancers, with amplification being the predominant mutation type. Notably, in Group 3 medulloblastoma, *LDHA* expression positively correlates with MYC amplification, suggesting *LDHA* inhibition as a potential therapeutic strategy [30]. Similarly, *LDHB* overexpression associates with KRAS copy number increases and mutations in lung cancer [31]. These findings collectively indicate that amplification-driven overexpression of *LDH* isoforms may serve as important oncogenic drivers and potential therapeutic targets.

Protein interaction network analysis demonstrated significant functional connections among *LDH* family members, with GO and KEGG enrichment analyses highlighting their involvement in key metabolic processes including lactate metabolism, pyruvate metabolism, and glycolysis/gluconeogenesis. These pathways play crucial roles in tumor biology, where pyruvate metabolism fuels cellular energy demands while lactate accumulation in the tumor microenvironment promotes immune evasion and supports malignant progression [32]. Our results suggest that *LDH*-mediated metabolic reprogramming may significantly contribute to CESC pathogenesis.

DNA methylation analysis revealed distinct epigenetic patterns among *LDH* isoforms in CESC. We observed hypermethylation of *LDHB* contrasting with hypomethylation of *LDHC*, both showing significant negative correlations with their respective expression levels. This finding aligns with existing literature demonstrating that *LDHA* promotes *HPV16* expression through *H3K79* methylation [33], while *LDHB* promoter methylation suppresses its tumor-suppressive function in breast and liver cancers [31] [34]. Interestingly, *LDHC's* demethylation pattern mirrors its testis-specific expression profile [35], supporting our hypothesis that methylation status regulates *LDH* isoform expression in tissue-specific manners. While direct evidence linking all *LDH* members to CESC remains limited, our findings strongly suggest that differential methylation contributes to tumorigenesis through metabolic pathway modulation.

Our immune correlation analysis uncovered complex relationships between *LDH* family members and tumor immunology. High *LDHA* expression correlated with poor patient survival, consistent with reports that *LDHA*-derived lactate accumulation impairs T cell and NK cell function in melanoma [36]. Similarly, *LDH*-related genes may promote CESC progression by activating M2 macrophages and inhibiting dendritic cell activation [37]. Immune checkpoint analysis revealed significant associations between *LDH* isoforms and key regulators including CTLA-4, PD-1, and PD-L1, which are critical targets for cancer immunotherapy [38] [39]. Notably, dual blockade of PD-L1 and *LAG3* demonstrates enhanced anti-tumor efficacy [40], suggesting potential combination strategies for CESC treatment.

Single-gene enrichment analysis implicated *LDHC* in the IL-17 signaling pathway, which plays established roles in inflammation and tumorigenesis [41]. While glycolytic genes typically promote tumor progression through IL-17 pathway activation [42], our functional studies revealed *LDHC*'s unexpected protective role in CESC. Knockout experiments demonstrated that *LDHC* depletion enhances tumor cell proliferation, migration, and invasion—a novel finding that challenges conventional understanding of *LDH* family functions. Although limited by the absence of in vivo validation and clinical sample constraints, these results position *LDHC* as a potential tumor suppressor in cervical carcinogenesis.

Our findings regarding the tumor-suppressive role of *LDHC* in CESC underscore the significant impact of the *LDH* family in the pathogenesis of gynecologic

malignancies. This observation aligns with recent studies emphasizing the critical and distinct functions of *LDH* isoforms. For instance, *LDHB* has been demonstrated to contribute to immune evasion in ovarian cancer cells [37], whereas *LDHA* plays a contrasting role in promoting the survival and proliferation of cervical cancer cells under energy stress conditions [43]. These collective findings indicate that the functional roles of the *LDH* family warrant further investigation. Future work should aim to elucidate whether the protective effect of *LDHC* is specific to the pathogenesis of CESC or represents a broader, previously unrecognized tumor-suppressive pathway in other gynecologic malignancies.

5. Conclusion

Our study establishes *LDHC* as a clinically significant biomarker in CESC, with high expression correlating with favorable outcomes. Functional characterization revealed its unique tumor-suppressive properties, as evidenced by enhanced malignant phenotypes following gene knockout. These findings provide novel insights into *LDH* family biology and suggest *LDHC* as a potential therapeutic target for cervical cancer management.

Acknowledgements

We appreciate the valuable suggestions from our colleagues on manuscript revision.

Author Contributions

Professor Dong and Professor Liao are responsible for the research design and writing guidance, while SX mainly participates in the experiment. SX and XZ are mainly involved in cell culture and statistical analysis. YH participated in the initial draft drafting and bioinformatics analysis. YL and ZX provide guidance for the experiment. All authors have made significant contributions to this article and have approved its submission.

Ethics Statement

The research pertaining to human tissues underwent a thorough examination and received approval from the Institutional Research Ethics Committee of Affiliated Hospital of Youjiang Medical University for Nationalities (Ethical review number: YYFY-LL-2023-145).

Funding

Funded by the Youth Fund Program of the Guangxi Natural Science Foundation (2023JJB140064) and the Project of Baise Scientific Research and Technology Development Plan in 2024 (Grant No. 20250321, 20250315).

Data Availability Statement

The data underlying in this study are freely available from the TCGA, GEO, GTEx,

GeneMANIA, STRING, Xiantao Academic, Home for Researchers, and HPA databases. All the original findings shown within the investigation are involved in the article/Supplementary Material. Regarding clinical trial number: Not applicable.

Conflicts of Interest

The authors declare no competing financial interests.

References

[1] Buskwofie, A., David-West, G. and Clare, C.A. (2020) A Review of Cervical Cancer: Incidence and Disparities. *Journal of the National Medical Association*, **112**, 229-232. https://doi.org/10.1016/j.jnma.2020.03.002

[2] Bosch, F.X., Lorincz, A., Munoz, N., Meijer, C.J.L.M. and Shah, K.V. (2002) The Causal Relation between Human Papillomavirus and Cervical Cancer. *Journal of Clinical Pathology*, **55**, 244-265. https://doi.org/10.1136/jcp.55.4.244

[3] Pujade-Lauraine, E. (2014) Editorial. *International Journal of Gynecological Cancer*, **24**, S1. https://doi.org/10.1097/igc.0000000000000266

[4] Cibula, D., Pötter, R., Planchamp, F., Avall-Lundqvist, E., Fischerova, D., Haie Meder, C., *et al*. (2018) The European Society of Gynaecological Oncology/European Society for Radiotherapy and Oncology/European Society of Pathology Guidelines for the Management of Patients with Cervical Cancer. *Radiotherapy and Oncology*, **127**, 404-416. https://doi.org/10.1016/j.radonc.2018.03.003

[5] Chargari, C., Peignaux, K., Escande, A., Renard, S., Lafond, C., Petit, A., *et al*. (2022) Radiotherapy of Cervical Cancer. *Cancer/Radiothérapie*, **26**, 298-308. https://doi.org/10.1016/j.canrad.2021.11.009

[6] Chiva, L., Zanagnolo, V., Querleu, D., Martin-Calvo, N., Arévalo-Serrano, J., Căpîlna, M.E., *et al*. (2020) SUCCOR Study: An International European Cohort Observational Study Comparing Minimally Invasive Surgery versus Open Abdominal Radical Hysterectomy in Patients with Stage IB1 Cervical Cancer. *International Journal of Gynecological Cancer*, **30**, 1269-1277. https://doi.org/10.1136/ijgc-2020-001506

[7] Small, W., Bacon, M.A., Bajaj, A., Chuang, L.T., Fisher, B.J., Harkenrider, M.M., *et al*. (2017) Cervical Cancer: A Global Health Crisis. *Cancer*, **123**, 2404-2412. https://doi.org/10.1002/cncr.30667

[8] Ferrall, L., Lin, K.Y., Roden, R.B.S., *et al*. (2021) Cervical Cancer Immunotherapy: Facts and Hopes. *Clinical Cancer Research*, **27**, 4953-4973. https://doi.org/10.1158/1078-0432.ccr-20-2833

[9] Sharma, S., Deep, A. and Sharma, A.K. (2020) Current Treatment for Cervical Cancer: An Update. *Anti-Cancer Agents in Medicinal Chemistry*, **20**, 1768-1779. https://doi.org/10.2174/1871520620666200224093301

[10] Akram, M. (2013) Mini-Review on Glycolysis and Cancer. *Journal of Cancer Education*, **28**, 454-457. https://doi.org/10.1007/s13187-013-0486-9

[11] Krieg, A.F., Rosenblum, L.J. and Henry, J.B. (1967) Lactate Dehydrogenase Isoenzymes—A Comparison of Pyruvate-to-Lactate and Lactate-to-Pyruvate Assays. *Clinical Chemistry*, **13**, 196-203.

[12] Kim, J.W., Tchernyshyov, I., Semenza, G.L., *et al*. (2006) HIF-1-Mediated Expression of Pyruvate Dehydrogenase Kinase: A Metabolic Switch Required for Cellular Adaptation to Hypoxia. *Cell Metabolism*, **3**, 177-185.

https://doi.org/10.1016/j.cmet.2006.02.002

[13] Pathria, G., Scott, D.A., Feng, Y., Sang Lee, J., Fujita, Y., Zhang, G., *et al*. (2018) Targeting the Warburg Effect via LDHA Inhibition Engages ATF 4 Signaling for Cancer Cell Survival. *The EMBO Journal*, **37**, e99735. https://doi.org/10.15252/embj.201899735

[14] Oyama, Y., Miyata, H., Shimada, K., Fujihara, Y., Tokuhiro, K., Garcia, T.X., *et al*. (2022) CRISPR/Cas9-Mediated Genome Editing Reveals 12 Testis-Enriched Genes Dispensable for Male Fertility in Mice. *Asian Journal of Andrology*, **24**, 266-272. https://doi.org/10.4103/aja.aja_63_21

[15] Wang, S., Xie, J., Li, J., *et al*. (2016) Cisplatin Suppresses the Growth and Proliferation of Breast and Cervical Squamous Cell Carcinoma Cell Lines by Inhibiting Integrin *β*5-Mediated Glycolysis. *American Journal of Cancer Research*, **6**, 1108-1117.

[16] Omolaoye, T.S., Omolaoye, V.A., Kandasamy, R.K., Hachim, M.Y. and Du Plessis, S.S. (2022) Omics and Male Infertility: Highlighting the Application of Transcriptomic Data. *Life*, **12**, Article 280. https://doi.org/10.3390/life12020280

[17] Wang, Y., Li, G., Wan, F., Dai, B. and Ye, D. (2018) Prognostic Value of D-lactate Dehydrogenase in Patients with Clear Cell Renal Cell Carcinoma. *Oncology Letters*, **16**, 866-874. https://doi.org/10.3892/ol.2018.8782

[18] Lyu, M., Gong, Y., Liu, X., Wang, Y., Wu, Q., Chen, J., *et al*. (2023) CDK7-YAP-LDHD Axis Promotes D-Lactate Elimination and Ferroptosis Defense to Support Cancer Stem Cell-Like Properties. *Signal Transduction and Targeted Therapy*, **8**, Article No. 302. https://doi.org/10.1038/s41392-023-01555-9

[19] Tomczak, K., Czerwińska, P. and Wiznerowicz, M. (2015) Review the Cancer Genome Atlas (TCGA): An Immeasurable Source of Knowledge. *Współczesna Onkologia*, **1**, 68-77. https://doi.org/10.5114/wo.2014.47136

[20] Saluja, R., Cheng, S., delos Santos, K.A. and Chan, K.K.W. (2019) Estimating Hazard Ratios from Published Kaplan-Meier Survival Curves: A Methods Validation Study. *Research Synthesis Methods*, **10**, 465-475. https://doi.org/10.1002/jrsm.1362

[21] Gao, J., Aksoy, B.A., Dogrusoz, U., Dresdner, G., Gross, B., Sumer, S.O., *et al*. (2013) Integrative Analysis of Complex Cancer Genomics and Clinical Profiles Using the Cbioportal. *Science Signaling*, **6**, 11. https://doi.org/10.1126/scisignal.2004088

[22] Warde-Farley, D., Donaldson, S.L., Comes, O., Zuberi, K., Badrawi, R., Chao, P., *et al*. (2010) The Gene MANIA Prediction Server: Biological Network Integration for Gene Prioritization and Predicting Gene Function. *Nucleic Acids Research*, **38**, W214-W220. https://doi.org/10.1093/nar/gkq537

[23] Rath, S., Sharma, R., Gupta, R., Ast, T., Chan, C., Durham, T.J., *et al*. (2021) Mitocarta3.0: An Updated Mitochondrial Proteome Now with Sub-Organelle Localization and Pathway Annotations. *Nucleic Acids Research*, **49**, D1541-D1547. https://doi.org/10.1093/nar/gkaa1011

[24] Chandrashekar, D.S., Karthikeyan, S.K., Korla, P.K., Patel, H., Shovon, A.R., Athar, M., *et al*. (2022) UALCAN: An Update to the Integrated Cancer Data Analysis Platform. *Neoplasia*, **25**, 18-27. https://doi.org/10.1016/j.neo.2022.01.001

[25] Chandrashekar, D.S., Bashel, B., Balasubramanya, S.A.H., Creighton, C.J., Ponce-Rodriguez, I., Chakravarthi, B.V.S.K., *et al*. (2017) UALCAN: A Portal for Facilitating Tumor Subgroup Gene Expression and Survival Analyses. *Neoplasia*, **19**, 649-658. https://doi.org/10.1016/j.neo.2017.05.002

[26] Liu, C.J., Hu, F.F., Xia, M.X., *et al*. (2018) GSCA Lite: A Web Server for Gene Set Cancer Analysis. *Bioinformatics*, **34**, 3771-3772.

[27] Goldberg, E., Eddy, E.M., Duan, C. and Odet, F. (2010) LDHC: The Ultimate Testis-Specific Gene. *Journal of Andrology*, **31**, 86-94. https://doi.org/10.2164/jandrol.109.008367

[28] Kong, L., Du, W., Cui, Z., Wang, L., Yang, Z., Zhang, H., *et al*. (2016) Expression of Lactate Dehydrogenase C in MDA-MB-231 Cells and Its Role in Tumor Invasion and Migration. *Molecular Medicine Reports*, **13**, 3533-3538. https://doi.org/10.3892/mmr.2016.4963

[29] Zhang, W., Wang, C., Hu, X., Lian, Y., Ding, C. and Ming, L. (2022) Inhibition of LDHA Suppresses Cell Proliferation and Increases Mitochondrial Apoptosis via the JNK Signaling Pathway in Cervical Cancer Cells. *Oncology Reports*, **47**, Article No. 77. https://doi.org/10.3892/or.2022.8288

[30] Tao, R., Murad, N., Xu, Z., Zhang, P., Okonechnikov, K., Kool, M., *et al*. (2019) MYC Drives Group 3 Medulloblastoma through Transformation of Sox2+ Astrocyte Progenitor Cells. *Cancer Research*, **79**, 1967-1980. https://doi.org/10.1158/0008-5472.can-18-1787

[31] McCleland, M.L., Adler, A.S., Deming, L., Cosino, E., Lee, L., Blackwood, E.M., *et al*. (2013) Lactate Dehydrogenase B Is Required for the Growth of Kras-Dependent Lung Adenocarcinomas. *Clinical Cancer Research*, **19**, 773-784. https://doi.org/10.1158/1078-0432.ccr-12-2638

[32] Liberti, M.V. and Locasale, J.W. (2016) The Warburg Effect: How Does It Benefit Cancer Cells? *Trends in Biochemical Sciences*, **41**, 211-218. https://doi.org/10.1016/j.tibs.2015.12.001

[33] Liu, Y., Guo, J., Liu, Y., Wang, K., Ding, W., Wang, H., *et al*. (2018) Nuclear Lactate Dehydrogenase a Senses ROS to Produce α-Hydroxybutyrate for HPV-Induced Cervical Tumor Growth. *Nature Communications*, **9**, Article No. 4429. https://doi.org/10.1038/s41467-018-06841-7

[34] Revill, K., Wang, T., Lachenmayer, A., Kojima, K., Harrington, A., Li, J., *et al*. (2013) Genome-wide Methylation Analysis and Epigenetic Unmasking Identify Tumor Suppressor Genes in Hepatocellular Carcinoma. *Gastroenterology*, **145**, 1424-1435.e25. https://doi.org/10.1053/j.gastro.2013.08.055

[35] Zhou, C., Zhang, L., Xu, D., Ding, H., Zheng, S. and Liu, M. (2022) MeDIP-Seq and RNA-Seq Analysis during Porcine Testis Development Reveals Functional DMR at the Promoter of LDHC. *Genomics*, **114**, Article 110467. https://doi.org/10.1016/j.ygeno.2022.110467

[36] Brand, A., Singer, K., Koehl, G.E., Kolitzus, M., Schoenhammer, G., Thiel, A., *et al*. (2016) LDHA-Associated Lactic Acid Production Blunts Tumor Immunosurveillance by T and NK Cells. *Cell Metabolism*, **24**, 657-671. https://doi.org/10.1016/j.cmet.2016.08.011

[37] Yang, X., Zhang, W. and Zhu, W. (2023) Profiling of Immune Responses by Lactate Modulation in Cervical Cancer Reveals Key Features Driving Clinical Outcome. *Heliyon*, **9**, e14896. https://doi.org/10.1016/j.heliyon.2023.e14896

[38] Zou, W., Wolchok, J.D. and Chen, L. (2016) PD-L1 (B7-H1) and PD-1 Pathway Blockade for Cancer Therapy: Mechanisms, Response Biomarkers, and Combinations. *Science Translational Medicine*, **8**, 328rv4. https://doi.org/10.1126/scitranslmed.aad7118

[39] Howitt, B.E., Sun, H.H., Roemer, M.G.M., Kelley, A., Chapuy, B., Aviki, E., *et al*. (2016) Genetic Basis for PD-L1 Expression in Squamous Cell Carcinomas of the Cervix and Vulva. *JAMA Oncology*, **2**, 518-522.

https://doi.org/10.1001/jamaoncol.2015.6326

[40] Shi, A., Tang, X., Xiong, Y., Zheng, K., Liu, Y., Shi, X., *et al*. (2021) Immune Checkpoint LAG3 and Its Ligand FGL1 in Cancer. *Frontiers in Immunology*, **12**, Article 785091. https://doi.org/10.3389/fimmu.2021.785091

[41] Li, X., Bechara, R., Zhao, J., McGeachy, M.J. and Gaffen, S.L. (2019) IL-17 Receptor–based Signaling and Implications for Disease. *Nature Immunology*, **20**, 1594-1602. https://doi.org/10.1038/s41590-019-0514-y

[42] Li, W., Xu, M., Li, Y., Huang, Z., Zhou, J., Zhao, Q., *et al*. (2020) Comprehensive Analysis of the Association between Tumor Glycolysis and Immune/Inflammation Function in Breast Cancer. *Journal of Translational Medicine*, **18**, Article No. 92. https://doi.org/10.1186/s12967-020-02267-2

[43] Jia, C., Wu, Y., Gao, F., Liu, W., Li, N., Chen, Y., *et al*. (2024) The Opposite Role of Lactate Dehydrogenase a (LDHA) in Cervical Cancer under Energy Stress Conditions. *Free Radical Biology and Medicine*, **214**, 2-18. https://doi.org/10.1016/j.freeradbiomed.2024.01.043